# A Forecasting Ionospheric Real-time Scintillation Tool (FIRST)

Rob Redmon (NOAA/NGDC)
David Anderson (Univ. of Colorado/CIRES and NOAA/SWPC)
Ron Caton (AFRL/RVXBI)
Terence Bullett (Univ. of Colorado/CIRES and NOAA/NGDC)

## I. Abstract

Trans-ionospheric radio waves propagating through an irregular ionosphere with plasma depletions, or "bubbles", are subject to sporadic enhancement and fading commonly referred to as scintillation. Knowledge of the current ionospheric condition allows system operators to distinguish between compromises due to the radio environment and system induced failures, while a forecast of the same provides the opportunity for operators to take appropriate actions to mitigate the effects and optimize service. This paper describes a technique that uses the readily accessible ionospheric characteristic h'F from ground based ionospheric sounder data near the geomagnetic equator to forecast the occurrence or non-occurrence of low latitude scintillation activity in VHF/UHF bands. We illustrate the development of the Forecasting Ionospheric Real-time Scintillation Tool (FIRST) and its real-time capability for forecasting scintillation activity. Finally, we have found that there exists a threshold in the h'F value at 19:30 LT that corresponds to the onset of scintillation activity in the Peruvian longitude sector which is found to decrease with decreasing F10.7 cm fluxes in a linear manner.

## II. Introduction

Communication and navigation systems can be severely disrupted due to the detrimental effects of scintillation on trans-ionospheric radio waves. The design and operation of high bandwidth space based VHF and UHF data and communications links, must consider these effects. Whenever signal strength is attenuated below the receiving system's fade margin, communications messages are compromised. In 1996, scintillation experiments were carried out at Ascension Island in which the message "THE QUICK BROWN FOX JUMPS OVER THE LAZY DOGS BACK 0123456789 TIMES" was repeatedly transmitted from Hanscom Air Force Base to Ascension Island. Figure 1 illustrates the degradation of SATCOM messages under varying degrees of scintillation intensity. During periods of scintillation, the received message was garbled. Taur (1973) first reported on the existence of equatorial plasma disturbances observed by the geosynchronous network INTELSAT. Since these early observations, many researchers have reported on various characteristics of low latitude plasma irregularity phenomenology. Irregularities with turbulent strength strong enough to produce scintillation events most typically occur between 20:00 and 03:00 local time (Basu, Su. et al., 1985; Chandra et al, 1993), with a dramatic increase in the occurrence rate of plasma bubbles after 1930 LT (Burke et al, 2004). In the Pacific sector, high activity occurs from March to June and from August to December, while in the American and African sectors, high activity occurs from September to April (Caton and Groves, 2006). High scintillation activity is most globally distributed during spring and fall equinox periods.

Even though solar cycle and magnetic activity strongly modulate scintillation strength and occurrence rate, it has been shown through observational studies that season (Tsunoda, 1985) and day-to-day variability during quiet conditions (Groves et al., 1997) are also significant modulators. Scintillation effects of bubble related F-region irregularities span across the magnetic equator, with occurrence rate maximized near the magnetic equator and scintillation intensity maximized near the anomaly crests or approximately +/- 15 degrees (Groves et al., 1997; Aarons and DasGupta, 1982; Kitner, 2007).

In this paper we relate the physical processes that occur in the equatorial ionosphere to the real-time operational forecasting of scintillation activity, which impacts communication and navigation customers. Figure 2 displays a schematic of the transport processes that are important in the low latitude ionosphere. In the low latitude, ionospheric F region, the ambient ion and electron density distributions are determined through the combined physical processes of production via impinging solar EUV radiation, loss of $O^+$ through charge exchange with molecular $N_2$ and $O_2$, transport along geomagnetic field lines by diffusion and neutral winds and transport perpendicular to **B** by **ExB** drift (Hanson and Moffett, 1966; Anderson, 1973). In the daytime E region (90 – 120 km), dynamo processes generate eastward electric fields, which are transmitted to F region altitudes (150 – 800 km) by equipotential geomagnetic field lines, causing both ions and electrons to drift upward perpendicular to **B** with a velocity equivalent to $\mathbf{ExB}/B^2$. At the same time, forces parallel to **B**, due to gravity and plasma pressure gradients, act to transport plasma down the magnetic field lines. The net effect is to create crests in electron density on either side of the magnetic equator at +/- 15 to 18 degrees dip latitude, known as the equatorial anomaly. Trans-equatorial neutral winds transport ionization from one hemisphere to the other causing asymmetries in both peak densities and peak altitudes in the equatorial anomaly.

The primary transport mechanism in creating the equatorial anomaly is the vertical **ExB** drift and Figure 3 displays the day-to-day variability in the vertical drifts as measured by the Jicamarca Incoherent Scatter radar (ISR) located at the magnetic equator in Peru (Scherliess and Fejer, 1999). Note the enhancement in upward **ExB** drift after 1800 LT just before downward drift commences. This is known as the pre-reversal enhancement (PRE) in **ExB** drift and is responsible for creating the ionospheric conditions conducive to the generation of small-scale plasma density irregularities in the ionosphere. In fact, the generation of equatorial, F-region plasma density irregularities, via the generalized Rayleigh-Taylor (R-T) instability mechanism is critically dependent on the magnitude of the PRE after sunset. The Rayleigh-Taylor (R-T) instability mechanism has been well-documented and discussed in Fejer and Kelley (1980) and Kelley (1989).

Recent investigations (Fejer et al. 1999, Fagundes et al. 1999) leave open the scientific question of whether an enhancement in upward **ExB** drift is necessary and sufficient or simply necessary for creating the ambient conditions conducive to scintillation activity. A campaign to study the day-to-day variability of scintillation activity and the corresponding measured vertical **ExB** drift velocities was carried out in the South American sector between September 25 and October 7, 1994 (Basu et al., 1996). The

Jicamarca Incoherent Scatter radar observed vertical **ExB** drift velocities while VHF (~250 MHz) receivers measured the scintillation activity $S_4$ index at Ancón, Peru and Aguaverde, Chile. Results from this campaign established that even a PRE in upward drift of only 20 m/sec during this solar minimum period, is a necessary condition for the development of scintillation activity.

More recently, Anderson et al. (2004) reported on the possibility of forecasting the occurrence of nightly scintillation activity at VHF/UHF frequencies in the equatorial ionosphere based on vertical **ExB** drift velocities at dusk. The primary objective of this study was to determine whether the pre-reversal enhancement in upward **ExB** drift is both necessary and sufficient or simply necessary for the development of irregularities in the nighttime ionosphere. They succeeded in establishing the relationship between the post-sunset vertical **ExB** drift velocity (1800-2000 LT) and the subsequent occurrence or non-occurrence of scintillation activity on a night-to-night basis. This study was carried out with data collected near the magnetic equator on the Western Coast of South America with sensors specifically positioned to 1) Infer vertical **ExB** drift velocities after sunset and 2) Observe the VHF scintillation $S_4$ index. SCINDA scintillation receivers located at Ancón, Peru and Antofagasta, Chile observed VHF radio signals from geostationary satellites and provided the $S_4$ Index. The Jicamarca, Peru Digisonde was used to observe the post-sunset height rise of the bottom-side F layer allowing the authors to infer the enhancement in upward **ExB** drift. They found that for the solar maximum years, 1998 and 1999, there existed a "threshold" of 20 m/sec in the vertical **ExB** drift velocity such that, below this value, $S_4 < 0.5$ and above this value $S_4 > 0.5$. For Antofagasta west observations, when **ExB** drift is greater than 20 m/sec, a "forecast" that the subsequent $S_4$ value would be >0.5 would be correct 92% of the time. Similarly, when the **ExB** drift was less than 20 m/sec, a forecast that $S_4$ would be <0.5 would be correct 85% of the time. Near the magnetic equator at Ancón, Peru the two corresponding percentages are 64% and 85%, respectively. Figure 4 illustrates this technique for inferring the PRE in the ExB drift velocity by observing the 4 MHz ($N_e = 2 \times 10^5$ el./cm$^3$) height-rise-with-time on October 12, 2009, resulting in an inferred upward drift of 10.7 m/s.

## III. Objective

This present study develops the capability to forecast regional VHF scintillation activity on a night-to-night basis through the use of ground-based ionospheric sounder observations near the magnetic equator. It has already been established that a "threshold" in the PRE **ExB** drift velocity exists that might be used for this forecast. However, a more easily accessible, real-time, ground-based sounder parameter, h'F has been found to be a suitable proxy for the **ExB** drift velocity. The ionospheric characteristic h'F is defined as the virtual height of the bottom-side F-layer. The value of h'F at 19:30 LT reflects the integrated upward **ExB** drift effect of lifting the F-layer to an altitude where the R-T instability mechanism becomes important. Choosing an h'F value at 1930 LT essentially integrates the effect of the **ExB** drift velocity in raising the F layer to a sufficiently high altitude where the R-T instability mechanism generates plasma density irregularities and scintillation activity. Figure 5 demonstrates the strong linear relationship between h'F values at 1930 LT and the peak PRE **ExB** drift velocities for 30 randomly selected, equinoctial, geomagnetically quiet days between 2002 and 2005. The peak PRE **ExB** drift values were determined using the height-rise-with-time technique illustrated in Figure 4 and the h’F values at 1930 LT were obtained from the Jicamarca sounder. The established relationship between a “threshold” in the **ExB** drift velocity and the occurrence or non-occurrence of scintillation activity and the linearity of the relationship between h’F (1930 LT) and the peak PRE **ExB** drift velocity support the idea that a “threshold” in h’F (1930 LT) and scintillation activity also exists.

There are 3 objectives to this study - 1) Demonstrate that there exists a “threshold” in the h’F virtual height at 1930 LT obtained by the ground-based digital sounder at Jicamarca, Peru and subsequent scintillation activity as evidenced by the Total Hourly Mean $S_4$ Index – THMS4 (Caton and Groves, 2006) from the SCINDA VHF scintillation receiver at Ancón, Peru, 2) Determine how the h’F (1930 LT) threshold altitude changes with solar activity (F10.7 cm flux) and 3) Develop a real-time, ionospheric scintillation activity forecast tool that is publicly available via a web browser or Google Earth application.

## IV. Approach

The justification for examining whether there exists a “threshold” in the h’F altitude, which can be used as a predictor of scintillation activity, lies in the fact that the ionospheric F layer has to attain a sufficiently high enough altitude after sunset, in order for the Rayleigh-Taylor (R-T) instability growth rate to be great enough to trigger development of irregularities. To fulfill this condition, the h'F altitude at 19:30 LT is used as a proxy, representing the integrated effect of upward **ExB** drift velocity after sunset. To determine the "threshold" h'F values, we used observations from the Jicamarca Digisonde to obtain daily h'F values at 19:30 LT for the months of 1) March-April, 2002; 2) March-April, 2003; 3) August-September, 2004 and 4) August-September, 2005. These were obtained from the University of Massachusetts Lowell Center for Atmospheric Research (UMLCAR), SAO Explorer version 3.4.0 from the Jicamarca, Peru Digisonde web site.

Radio signals passing through ionospheric regions where irregular plasma density structures exist, experience strong amplitude fluctuations called "scintillation". The Scintillation Index ($S_4$) is a measure of scintillation intensity and provides a way to observe the gross magnitude of satellite signal fluctuations. $S_4$ is defined as the normalized standard deviation of the signal intensity, over a selected time interval

$$S_4 = \left(\left\langle I^2 \right\rangle - \langle I \rangle^2\right) / \langle I \rangle^2$$

where brackets represent ensemble average, which can be approximated as the time average. Observations of scintillation activity are obtained from a network of VHF and L-band receivers established by the Air Force Research Laboratory in the South American sector (Groves et al., 1997) called the SCIntillation Network Decision Aid (SCINDA). At Ancón, Peru (11.8 S, 282.9 E) near the magnetic equator, SCINDA receivers record scintillation at VHF (~250 MHz) and L-Band (1.5 GHz) on signals received from communication satellites in geosynchronous orbit. Additionally, a GPS receiver measures scintillation on links to all GPS satellites in view. Each receiver samples the raw signals at 50-100 Hz. The data are processed on line to determine the statistical scintillation index, or $S_4$, over 60 second intervals. An identical receiver configuration is located in Antofagasta, Chile, (26.7 S, 289.6 E) under the southern equatorial anomaly crest. The Ancón and Antofagasta SCINDA installations were established in 1996 and currently run autonomously with the processed output streaming to AFRL every 15 minutes over dedicated lines.

## V. Results

This study investigates the relationship between the observed h'F values at 19:30 LT from the Jicamarca digital sounder and the Total Hourly Mean $S_4$ (THMS4) values obtained from the SCINDA VHF Ancón $S_4$ observations. The nightly THMS4 parameter is a derived quantity ranging from 0 to 5. It specifies both the intensity and duration of scintillation activity as measured from a ground station where a value of 1 indicates moderate activity and a value of 3-5 is an indication of more intense scintillation. While it has been shown that there exists a "threshold" in post-sunset **ExB** drift velocities that determine whether or not scintillation activity will occur, the important parameter is the height of the F layer since this has been shown by Sultan (1996) and others to critically affect the R-T growth rate values. Thus, this study investigates the relationship between the observed h'F values at 19:30 LT from the Jicamarca digital sounder and the subsequent THMS4 values obtained from the SCINDA VHF Ancón observations. The advantage of using readily available h'F values at 19:30 LT lies in the fact that the height of the F layer is the more critical parameter to associate with R-T growth rates. It is important to determine whether a “threshold” exists in h’F relating to the occurrence (or non-occurrence) of scintillation as. This has already been shown with post-sunset **ExB** drift values (Anderson et al., 2004).

We have compared the THMS4 values obtained from Ancón VHF observations with the h’F values at 19:30 LT from the Jicamarca sounder for several pairs of months in 2002, 2003, 2004, 2005 and 2008. We have qualitatively determined the “threshold” values of h’F values (h’$F_{thr}$) which seem to act as demarcation markers for nightly THMS4 values significantly less than 1, indicative of low scintillation activity, and those significantly greater than 1, indicative of stronger scintillation levels. Figure 6 plots the “threshold” h’F values for 2002, 2003 and 2004 and all of the THMS4 values obtained for the pairs of months. The h’F threshold values for 2002, 2003 and 2004 are, respectively, 400, 340 and 310 km. The average F10.7 cm flux for each of the pairs of months has been determined and Figure 7 displays the linear relationship that exists between the threshold h’F altitudes and the month-pair averaged F10.7 cm flux from 2002 to 2008. The relationship between h’$F_{thr}$ and this average F10.7 cm flux has an $R^2 = 0.99$ and is given by:

$$h'F_{thr}\ (19{:}30\ \mathrm{LT}) = 1.14 \times F10.7 + 192.7$$

The blue squares plotted in Figure 7 represent the altitude where the density of atomic oxygen [O] is 2.5 x $10^8$ parts/$cm^3$ from the MSIS neutral atmosphere model. While the h’$F_{thr}$ vs. F10.7 cm flux slope is not identical to the [O] = 2.5 x $10^{8}$ $cm^{-3}$ vs. F10.7 cm flux slope, the similarity between the two establishes that the R-T threshold growth rate ($\gamma$ (R-T) ~ $g/\nu_{in}$) occurs at a lower altitude with decreasing F10.7 cm flux values because the same ion-neutral collision frequency ($\nu_{in} \sim [O]$) occurs at decreasing altitudes with decreasing F10.7 cm flux values.

Our analyses thus far have focused on the Jicamarca, Peru region. The Kwajalein Atoll, located at ~4 degrees magnetic latitude (9N, 167.2E) in the Pacific region, is another area of interest. Neutral atmospheric properties at Kwajalein and Jicamarca are expected to be similar.

Theoretical ionospheric models predict a similar variation of the threshold with solar activity. PBMOD, the Physics-Based Model developed at the Air Force Research Laboratory (Retterer, 2005), was run for the Kwajalein longitude to determine the drift thresholds for scintillation activity and the state of the ionosphere at the threshold (Retterer and Gentile, 2009) for solar fluxes of 80 and 180. John Retterer (private communication) found that the height of the lower edge of the F layer (looking at the height of the maximum vertical density gradient, which is close to but not exactly the same as h'F) at the threshold varied with solar flux in much the same way as h'F does in Figure 7.

**VI. Operational Forecasting**

The post-sunset h'F "threshold" results are used to create nightly scintillation forecasts for the equatorial ionosphere in the American (Jicamarca, Peru) and Pacific (Kwajalein Atoll) sectors. While the American sector forecast is justified by the arguments of this paper, further validation will be performed on the Pacific sector forecasts using truth data sets collected on SCINDA receivers located on Kwajalein Atoll. Bottom-side ionospheric soundings are recorded at the Jicamarca and Kwajalein ionosonde observatories with a cadence of 15 minutes and 5 minutes respectively. These recordings use an automatic scaling algorithm to characterize the minimum height of the F layer, h'F, upon which the aforementioned scintillation forecast technique is based. These observations are then transmitted in near real time to World Data Center “A” at the NOAA National Geophysical Data Center under the auspices of the Solar and Terrestrial Physics Division. Forecasts are then produced for each evening beginning with an early forecast at 18:30LT, and continuing with an updates every 15 minutes through 19:30LT. The idea is to begin forecasting once the probability of a false positive (scintillation likely event) is reasonably small and continually update the forecast as new real time observations become available. In this manner, early warnings are made possible, and the forecast is continually improved. A forecast is color coded as “Red” for “Scintillation Likely”, “Yellow” for “Scintillation Possible” and “Green” for “Scintillation Unlikely.” In terms of h’F values observed at 19:30 LT, Table 1 gives the definition of the Red, Yellow and Green forecasts.

| Color | Red | Yellow | Green |
|---|---|---|---|
| Meaning | *Likely* | *Possibly* | *Unlikely* |
| h’F Range | $h'F > (h'F_{thr} + 10)$ | $(h'F_{thr} + 10) > h'F > (h'F_{thr} - 10)$ | $h'F < (h'F_{thr} -10)$ |

Table 1: FIRST color-coded scintillation thresholds.

These daily forecasts are publicly accessible through three internet interfaces: 1) Google Earth, 2) Web Browser, and 3) FTP. The Google Earth tool provides the current space weather for many real time stations along with scintillation forecasts for Jicamarca and Kwajalein. The web browser product shows a simplified view of the scintillation forecast. This product was specifically developed to be hand held device friendly (e.g. Blackberry, iPhone) or incorporated into another web page. The FTP data service provides access to the forecast, as well as a running comparison of the FIRST forecasts and direct SCINDA scintillation measurements. Figure 8 displays the h'F-observed values for the Jicamarca sounder for local times between 18:30 and 19:30 LT and days between October 14 (day 287) and October 8 (day 281). The h'F values are coded "Red", "Yellow" or "Green" depending on whether the values are above 270 km, between 270 and 250 km and below 250 km, respectively. Similarly, Figure 9 displays the same information obtained by the Kwajalein. In both cases, a blue "N/A" indicates that data was not available near the local time in question, while a "*" next to a forecast value indicates that interpolation between two neighboring observation times was performed to yield a uniform forecast time. Figure 10, shows a typical forecast displayed on a portable device.

## VII. Conclusions

Communications and navigation systems can be severely disrupted due to the detrimental effects of scintillation on transionospheric radio waves. The pre-reversal enhancement (PRE) of the vertical **ExB** drift is the dominant sunset process driving the height of the F layer upward. This paper has demonstrated that in the Peruvian longitude sector, there is an excellent correlation ($R^2 \sim 0.91$) between the maximum PRE as determined by the height-rise-with-time of the 4 MHz ($2x10^5$ el/cm$^3$) contour (observed by the Jicamarca Digisonde) and the Digisonde-observed h'F value at 19:30 LT. We also find there to be a "threshold" value in h'F (19:30 LT) above which the nightly computed VHF scintillation activity index, THMS4, is greater than 1 and below which, THMS4 is less than 1. In addition, this h'F threshold value, $h'F_{thr}$, decreases with decreasing F10.7 cm flux. The linear relationship between $h'F_{thr}$ and F10.7 cm flux is given by,

$$h'F_{thr}\ (19{:}30\ LT) = 1.14 \text{ x } F10.7 \text{ cm flux} + 192.7$$

Based on this relationship, a real-time, forecasting technique has been developed for the Peruvian and the Kwajalein Atoll longitude sectors. The FIRST system, automatically acquires h'F values between 18:30 and 19:30 LT in real time from the ground-based sounders at Jicamarca, Peru and the Kwajalein Atoll and computes a forecast for the evening. Forecasts are made publicly available to Google Earth, portable devices and web browsers. For more information, please visit the FIRST web page located at http://ngdc.noaa.gov/stp/IONO/FIRST.html

**VIII. Acknowledgements**

The authors wish to thank Trevor Garner of the Space and Geophysics Laboratory Applied Research Laboratories at the University of Texas at Austin for his valuable suggestions during the drafting of this manuscript; Jorge Chau of the Jicamarca Radio Observatory (JRO), and Dale Sponseller and Robert Ferguson of Kwajalein Range Services for maintaining excellent ionosonde observatories at Jicamaraca and Kwajalein respectively.

## IX. References

Aarons, J., Dasgupta, A. (1982), Global morphology of ionospheric scintillations, *Proc. IEEE*, 70, 360-378.

Anderson, D. N. (1973). A theoretical study of the ionospheric F region equatorial anomaly, 2. Results in the American and Asian sectors, *Planet. Space Sci, 21*, 421- 442.

Anderson, D. N., B. Reinisch, Valladares, C., Chau, C., Veliz, O. (2004). Forecasting the occurrence of ionospheric scintillation activity in the equatorial ionosphere on a day-to-day basis, *Journal of Atmospheric and Solar-Terrestrial Physics*, Volume 66, Issue 17, Pages 1567-1572, ISSN 1364-6826, DOI: 10.1016/j.jastp.2004.07.010.

Basu, S. et al. (1996), Scintillation, plasma drifts, and neutral winds, *J. Geophys. Res., 101,* 26,795-26,809.

Basu, Su. (1985), Equatorial F region irregularities, in Handbook of Geophysics and the Space Environment, edited by A. S. Jusra, 9.3.5, Air Force Geophys. Lab., Hanscom AFB, Mass.

Burke, W. J., C. Y. Huang, et al. (2004). "Seasonal-longitudinal variability of equatorial plasma bubbles." Annales Geophysicae 22(9): 3089-3098.

Caton R., K. Groves (2006), Longitudinal correlation of equatorial ionospheric scintillation, *Radio Sci*., 41, RS5S22, doi:10.1029/2005RS003357.

Chandra, H., G. D. Vyas, et al. (1993). "Coordinated Multistation Vhf Scintillation Observations in India During March-April 1991." Indian Journal of Radio & Space Physics 22(2): 69-81.

Fagundes, P. R., Y. Sahai, I. S. Batista, M. A. Abdu, J. A. Bittencourt, H. Takahashi (1999), Observations of day-to-day variability in precursor signatures of equatorial F-region plasma depletions, *Ann. Geophysicae, 17,* 1053-1063.

Fejer, B. G., and M. C. Kelly (1980), Ionospheric irregularities, *Rev. of Geophys, 18*, 401-450, 1980.

Fejer, B. G., L. Scherleiss and E. R. de Paula (1999), Effects of the vertical plasma drift velocity on the generation and evolutions of equatorial spread-F., *J. Geophys. Res., 104*, 19859 – 19869.

Groves, K. M., S. Basu, E. J. Weber, M. Smitham, H. Kuenzler, C. E. Valladares, R., Sheehan, E. MacKenzie, J. A. Secan, P. Ning, W. J. McNiell, D. W. Moonan, M. J. Kendra (1997), Equatorial scintillation and systems support, *Radio Science, 32,* 2047-2064, 1997.

Kelley, M. C. (1989), The Earth's Ionosphere, *Int. Geophysical Series*, Vol. 43, Academic Press, San Diego, Calif.

Kitner, P. M. (2007), GPS and ionospheric scintillations, *Space Weather*, 5, S090003, doi:10.1029/2006SW000260.

Hanson, W. B., and R. J. Moffett (1966), Ionization transport effects in the equatorial F region, *J. Geophys. Res.*, *71*, 5559-5572.

Retterer, J. M. (2005), Physics-based forecasts of equatorial radio scintillation for the Communication and Navigation Outage Forecasting System (C/NOFS), *Space Weather*, 3, S12C03, doi:10.1029/2005SW000146.

Retterer, J. M., and L. C. Gentile (2009), Modeling the climatology of equatorial plasma bubbles observed by DMSP, *Radio Sci.*, *44*, RS0A31, doi:10.1029/2008RS004057.

Scherliess, L. and B. G. Fejer (1999), Radar and satellite global equatorial F region vertical drift model, *J. Geophys. Res*., *104,* 6829-6842.

Sultan, P. J. (1996). Linear theory and modeling of the Rayleigh-Taylor instability leading to the occurrence of equatorial spread F, *J. of Geophys.* Res, 101(A12): 26875-26891.

Taur, R. R. (1973), Ionospheric scintillation at 4 and 6 GHz, COMSAT Technical Review, 3, 145, 1973.

Tsunoda, R. T. (1985), Control of the seasonal and longitudinal occurrence of equatorial scintillations by the longitudinal gradient in integrated E region Pedersen conductivity, *J. Geophys. Res.*, 90, 447-456.

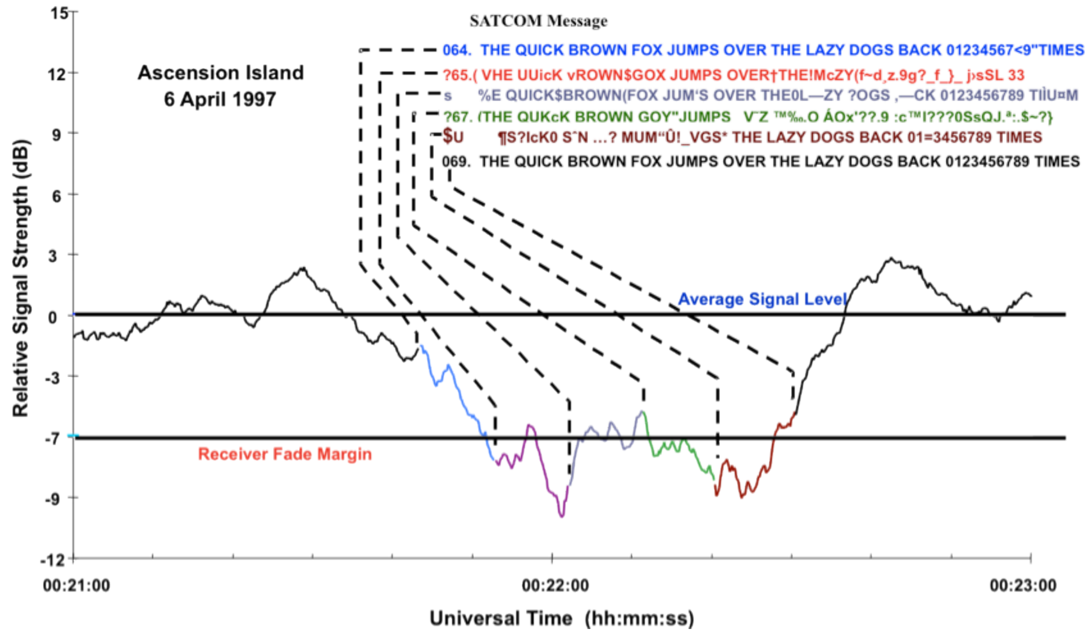


*Figure 1: A real-world example of SATCOM effects from an AFRL campaign in 1997. During periods of scintillation, the received message at Ascension Island was garbled.*

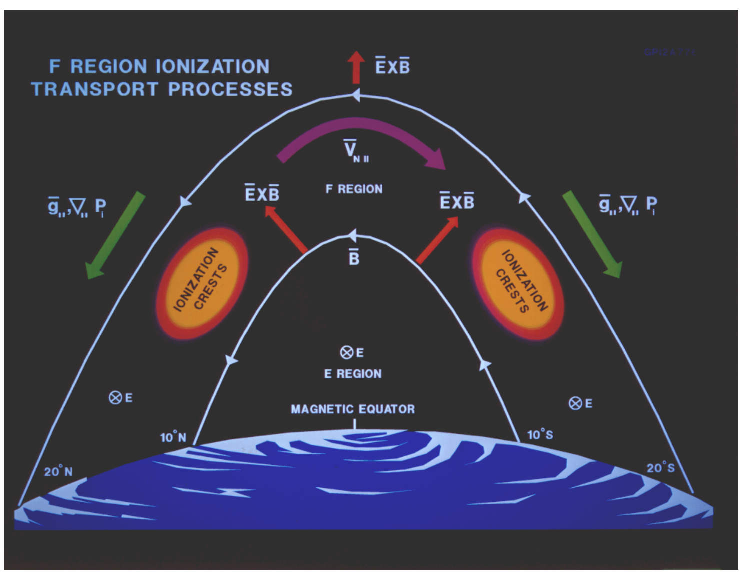


*Figure 2: Schematic of F-region ionization transport processes.*

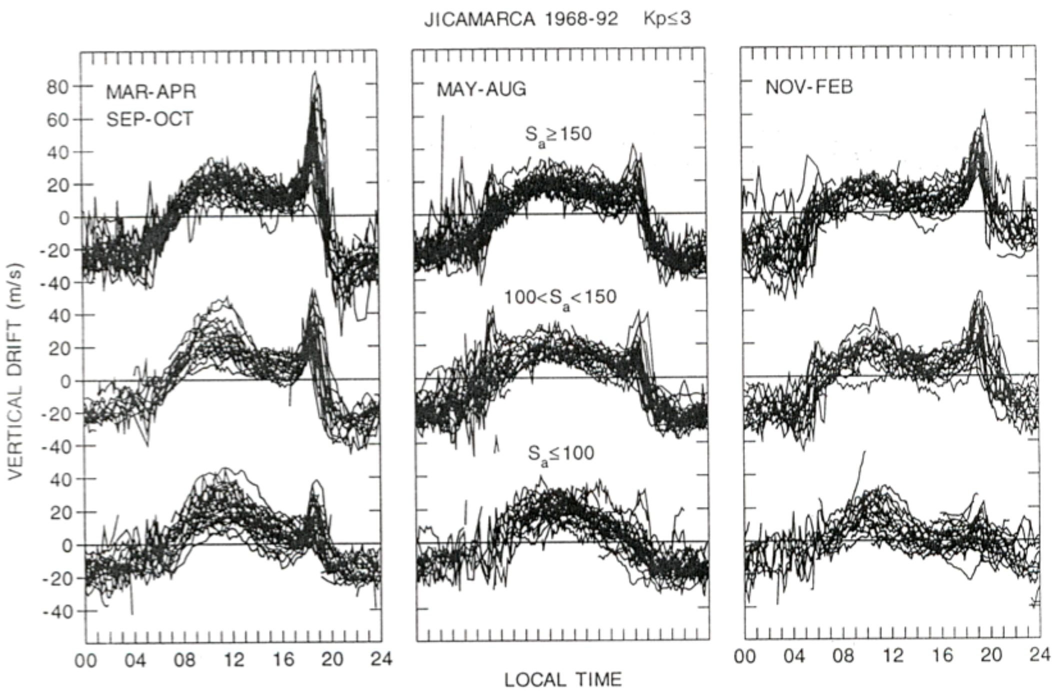


*Figure 3: Day-to-day variability in vertical ExB drift velocities as a function of local time, season and solar activity.*

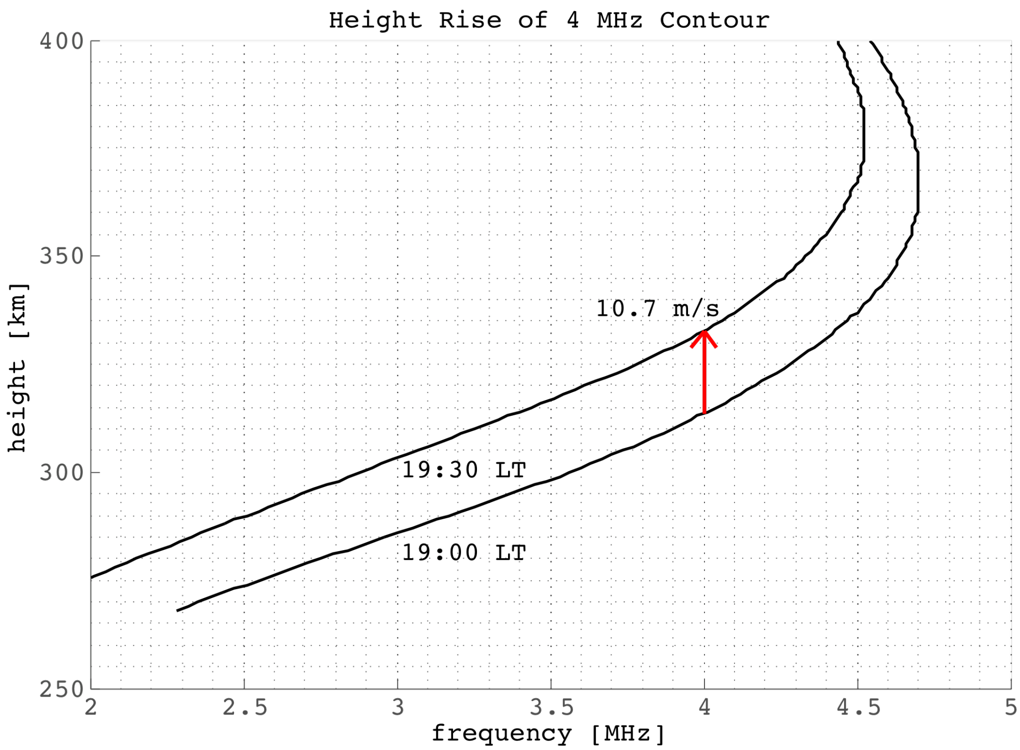


*Figure 4: The height-rise with time of the 4 MHz contour between 19:00 and 19:30 LT at Jicamarca on October 12, 2009, resulting in an inferred upward drift of 10.7 m/s.*

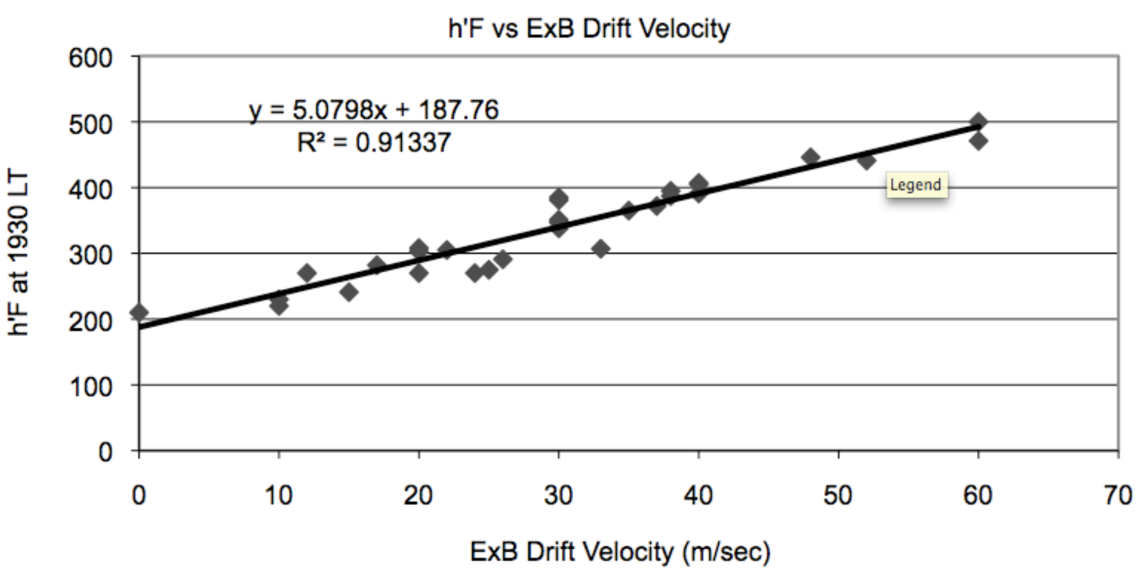


*Figure 5: h'F virtual height at 19:30 LT vs. the PRE ExB drift velocities for 30 days between 2002 and 2005.*

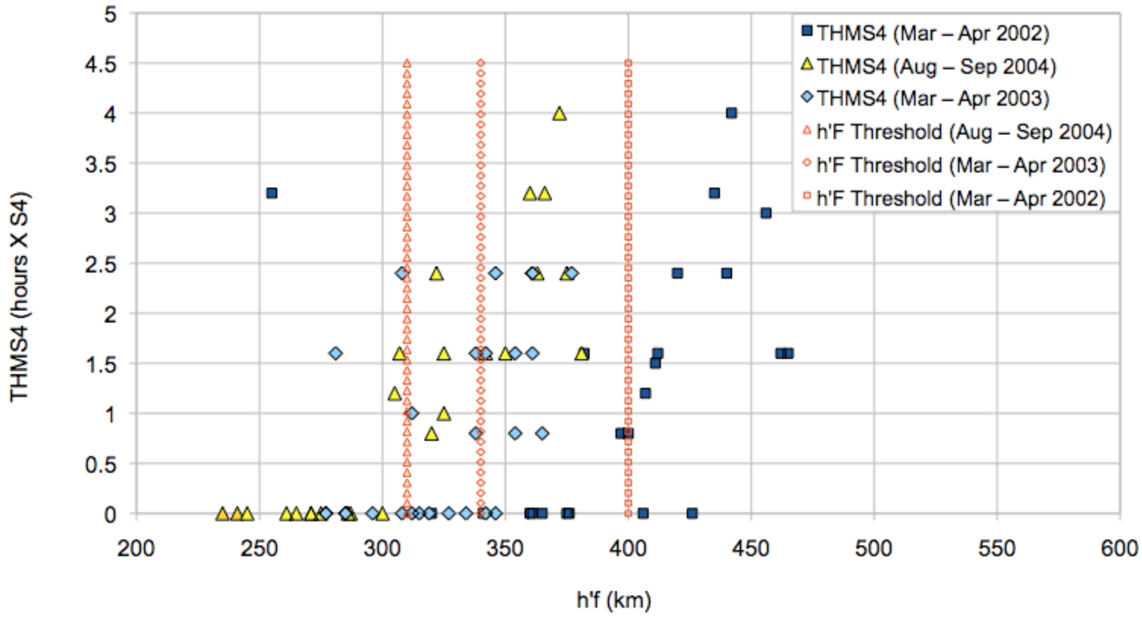


*Figure 6: Estimated "threshold" h'F values for 2002, 2003 and 2004.*

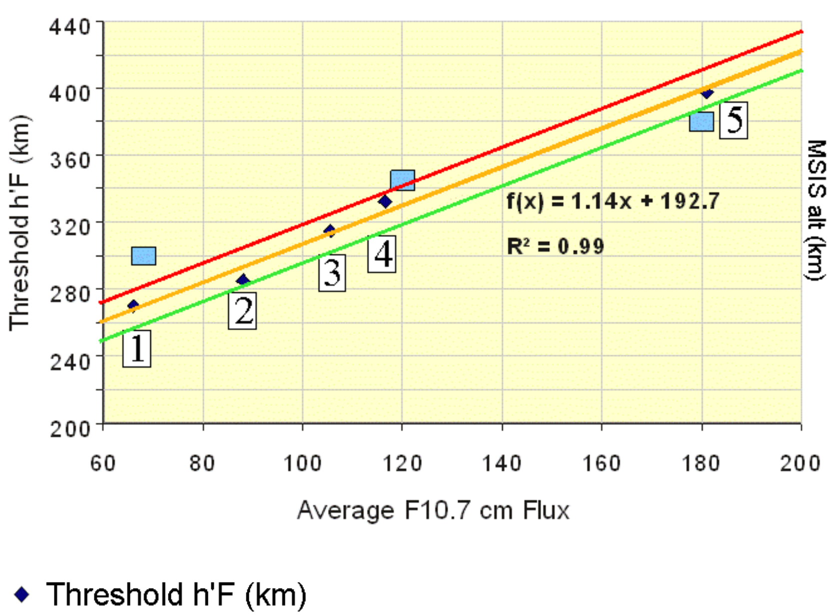

MSIS altitude when [0] = $2.5 \times 10^8$ $cm^{-3}$

*Figure 7: Threshold h'F values vs. F10.7 cm flux values for [1] 2008 (Aug, Sep), [2] 2005 (Aug, Sep), [3] 2004 (Aug, Sep), [4] 2003 (Mar, Apr) and [5] 2002 (Mar, Apr).*

**Jicamarca Scintillation Forecast (FIRST)**

h'F time history (LT):

| Date | 10/14 | 10/13 | 10/12 | 10/11 | 10/10 | 10/9 | 10/8 |
|---|---|---|---|---|---|---|---|
| Day of Year | 287 | 286 | 285 | 284 | 283 | 282 | 281 |
| 19:30LT | 260 | 260 | 320 | 250 | 280 | 255 | 256 |
| 19:15LT | 263 | 265 | 300 | 251 | 290 | 255 | 247 |
| 19:00LT | 255 | 262 | 298 | 250 | 262 | 255 | 240 |
| 18:45LT | 252 | 251 | 278 | 250 | 245 | 247 | 236 |
| 18:30LT | 250 | 247 | 267 | 247 | 235 | 246 | 230 |
| THMS4 | 1.29 | 1.67 | 1.06 | 0.21 | 1.12 | 1.02 | 0.45 |

*Figure 8: Jicamarca Scintillation Forecast for October 8 through October 14, 2009.*

**Kwajalein Scintillation Forecast (FIRST)**

h'F time history (LT):

| Date | 10/14 | 10/13 | 10/12 | 10/11 | 10/10 | 10/9 | 10/8 |
|---|---|---|---|---|---|---|---|
| Day of Year | 287 | 286 | 285 | 284 | 283 | 282 | 281 |
| 19:30LT | 280* | 300 | 245 | 258* | 210 | 225 | 285 |
| 19:15LT | 305 | 290* | 245 | 250* | 242* | 220 | 248* |
| 19:00LT | N/A | 282* | 253* | 245 | 237* | 220 | N/A |
| 18:45LT | 285 | 270* | 270 | 248* | 225 | 220 | 260 |
| 18:30LT | 335 | 235 | 248* | 185 | 220 | N/A | 260 |
| THMS4 | 1.47 | 0.13 | 0.11 | 0.09 | 0.1 | 0.33 | 0.16 |

*Figure 9: Kwajalein Scintillation Forecast for October 8 through October 14, 2009.*

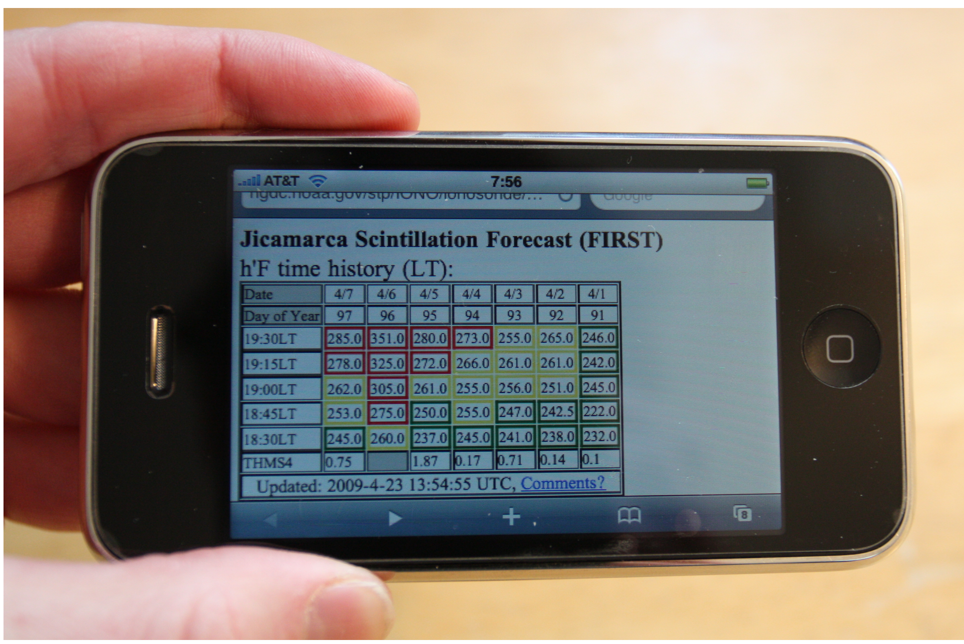


*Figure 10: PDA accessible Jicamarca Scintillation Forecast for April 1 through April 7 (LT), 2009.*